Seismic Ductility of Base Isolated Structures

by

Antonio Occhiuzzi
Ingegnere, Universita' degli Studi "Federico II", Napoli, Italia (1989)

Submitted to the Department of Civil and Environmental Engineering in Partial Fulfillment of the Requirements for the Degree of

Master of Science in Civil and Environmental Engineering

at the

MASSACHUSETTS INSTITUTE OF TECHNOLOGY

May 1994

Author .....
Department of Civil and Environmental Engineering
Submitted on May 13, 1994

Certified by .....
Daniele Veneziano, Professor of Civil Engineering
Department of Civil and Environmental Engineering
Thesis Supervisor

Accepted by .....
Joseph M. Sussman, Chairman
Departmental Committee on Graduate Studies

Seismic Ductility of Base Isolated Structures

by

Antonio Occhiuzzi

Submitted to the Department of Civil and Environmental Engineering of the Massachusetts Institute of Technology on May 13, 1994, in partial fulfillment of the requirements for the degree of Master of Science

Abstract

Ductility-based structural design is adopted by almost all seismic codes of the world. The damage potential of conventional, fixed-base structures has been thoroughly studied by many researchers, and the state-of-art knowledge of this subject is reflected into the reduction factors provided by many codes. Base isolation is today on the cutting edge of seismic-resistance engineering, as evidenced by the rapidly increasing number of buildings using this technique for new constructions and retrofit. Evidences of loss of ductility in base-isolated structures, however, abound in literature, but the analyses published do not provide simple, general ways to evaluate appropriate reduction factors. In this thesis, simple methods based on equivalent linearization and modal analysis are used to explain and quantify the seismic ductility of multi-degree-of-freedom base-isolated systems. Comparison with fixed-base structures are presented, and conclusions are drawn on the safety checking format and the response modification factors.

Thesis Supervisor: Daniele Veneziano
Title: Professor of Civil Engineering, Massachusetts Institute of Technology

Acknowledgment

The study presented in this thesis has been carried out under the supervision of professor Daniele Veneziano, whose guidance and support have gone well beyond the usual academic relationship between instructor and student.

Every single time I managed to work out the various problems I encountered in this thesis, I felt in debt with professor Aldo Raithel for having provided me with the cultural background needed.

The program of study at the MIT and therefore this thesis have been possible partially by the financial support of the "Dottorato di Ricerca" fellowship granted by the Italian Government (Ministero dell'Universita' e della Ricerca Scientifica).

Questa tesi e' dedicata a mia madre e a mio padre, e a Marina: senza di loro, questa meravigliosa avventura sarebbe rimasta solo un bellissimo sogno.

Biographical Notes

Antonio Occhiuzzi graduated in Civil Engineering at the University "Federico II" of Naples, Italy, in 1989. After the graduation, he got the position of on-site chief engineer in the development and construction of an urban sewer. Thereafter, he worked as structural engineering consultant until he won the public competition to be admitted to the Ph.D. program in Structural Engineering at the University "Federico II" of Naples, Italy. He is co-author of more than 10 papers dealing with various aspects of structural engineering.

Table of Contents

Chapter 1

Introduction

Base isolation has proven to be one of the most promising technique for seismic protection of buildings. The concepts behind the technique reflect the change in the conceptual approach to seismic design, from only providing sufficient safety to also ensure serviceability and economical reliability, at least for strategically important buildings (Kelly, 1993). For controlling the structural response and damage under ground motions of moderate to medium intensities, base isolation offers noticeable advantages compared with conventional, fixed-base design. A major problem to be solved, however, is to determine the level of protection that this technology provides against major structural damage and collapse. The clearly known mechanism according to which ductility develops in fixed-base (FB) structures allows the definition of response reduction factors (R_{WI} factors in the UBC code, q factors in the Eurocode) to be adopted in linear-based design codes. Evidences of reduced post-yielding seismic resistance in base-isolated (BI) structures abounds (Kaneko et al. 1990; Vestroni et al., 1991; Lin and Shenton, 1992; Calderoni et al., 1993). However, a simple, general way to estimate the structural capacity of base-isolated structures has not been proposed yet. In fact, although the reduction factors are generally lower for BI structures than for FB structures, there is not a general agreement on the currently proposed values.

The main objective of this thesis is to study the most important parameters influencing seismic demand in BI structures. An extensive investigation of the seismic response of isolated structural systems under various seismic inputs has been carried out. Time step integration has been discarded as a method to calculate structural response, in favor of

Chapter 2

Seismic Design of Fixed Base and Base Isolated structures

2.1 Fixed-Base Structures

In conventional, FB structures, the almost universally accepted design concept is that seismic resistance must be obtained by dissipating the energy fed by the ground motion through inelastic deformation of the structural members (Stanton and Roeder, 1991). This concept is implemented by codes trough the response modification factors, or response reduction factors R, which reduce the level of ground motion to be resisted elastically. Reduction factors are found in almost all seismic design codes: sometimes they are explicitly given, in other cases they are implicit in prescribed scaled down versions of the design response spectra.

Conceptually, the choice of R should depend on the available structural ductility and the additional strength (overstrength) beyond first yielding (Bertero, 1986; Bertero 1988). These parameters are the most important ones affecting the damage potential of earthquakes on nonlinear structures. The reduction factors suggested by codes are determined on the basis of theoretical studies carried out by many researchers, empirical engineering judgement (De Luca et al., 1994) and cost considerations. They usually reflect the concept that a tolerable amount of damage is allowed, under a relatively mild design basis earthquake (DBE), whereas extensive damage but no loss of human lives are acceptable under the maximum credible earthquake (MCE) for the site considered. The latter condition, however, is only implicitly considered by codes, because no structural assessment under the MCE is generally required.

3. For given magnitude and epicentral distance, the coefficient of variation of F is typically much lower than that of the elastic spectrum ordinates at the pre-yield natural period and damping ratio.

2.2 Base-Isolated Structures

The extension of seismic ductility design to BI structures is not straightforward. The main objective of isolating a building is not to excite the dynamic mode of the superstructure. This objective can be achieved by reducing the stiffness of the isolation system to levels much below those of the superstructure. In order to reduce the displacements of the relatively "soft" isolation layer, a high level of energy dissipation, through viscous or hysteretic damping, is introduced in the isolation system. Due to the nonlinear behavior of both the isolation system and the superstructure, ideal isolation cannot be attained for all levels of excitations and the isolation system is typically designed for the DBE. Once the DBE is exceeded, BI structures tend to develop inelastic deformations more rapidly than FB structures. Evidence of this loss of ductility abounds in literature, but published analyses rarely go beyond consideration of a few cases studies and no simple way to evaluate F is available. Current codes on BI structures suggest reduction factors much lower than those adopted for FB structures to account for this "brittle" behavior: however, their physical meaning, or their rationale, is unclear, reflecting the general disagreement in the scientific community on that subject.

Economical and social consideration are going to play a significant role in the development of BI structure design and construction. The concept of tolerable structural damage under the DBE has proven not to necessarily produce optimal structural design: even if losses of human lives have been drastically reduced in recently constructed or retrofitted civil structures, the high costs for repairing both the structures and their content make administrations and scientists wonder if more conservative design can lead to overall

Chapter 3

Equivalent Linearization Methods in the Analysis of Base Isolated Structures

3.1 Linearized Analysis

The main objective of this thesis is to investigate the seismic behavior, and in particular the ductility demand, of base isolated structures. In order to understand the factors that influence such behavior, a comprehensive investigation has been carried out, and the results are presented in the following Chapter 4. Although technically feasible, time step integration has not been used as too time consuming and therefore limiting the breadth of the analysis. Rather, a linearization technique combined with modal superposition has been used for both fixed-base and base-isolated structures. In the following, various linearization techniques are presented. A procedure to evaluate modal damping ratios in the presence of different structural materials is also described.

3.2 Secant Stiffness Linearization

Almost all the Design Codes that cover base isolated structures suggest a linearization procedure based on the concept of secant stiffness. These include the SEAOC-1990 *blue book*, the UBC-1991 and the AASHTO-1992 design codes, as well as the code recently proposed in Italy (Servizio Sismico Nazionale Italiano, 1993). Although secant linearization is a well known method, it is interesting to analyze its implications in terms of both stiffness and loss factors, relative to other linearization techniques. For this purpose, consider the bilinear hysteretic force-displacement relationship in fig. 3.1, in which the following symbols are used:

x	displacement	K_1	initial stiffness
x_y	yielding displacement	K_2	post-yielding stiffness
F	restoring force	K_s	secant stiffness
F_y	yielding force		

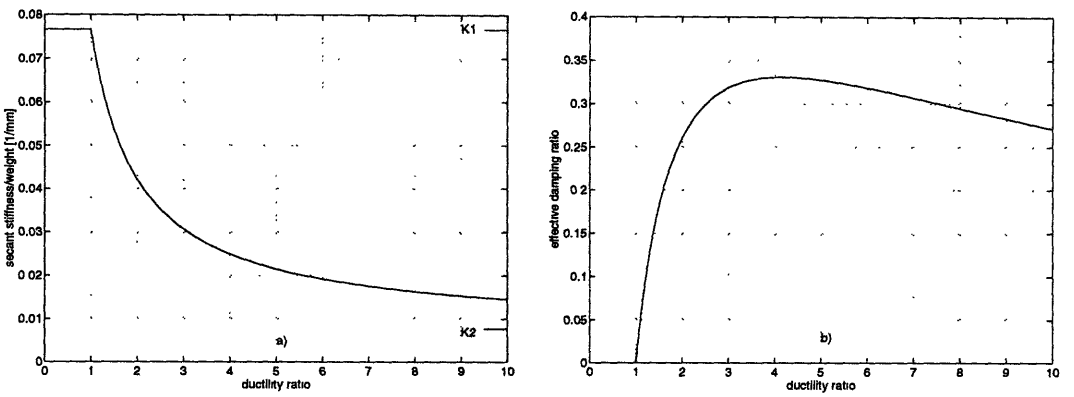

Figure 3.2: a) secant stiffness vs. ductility ratio; b) effective damping ratio vs. ductility ratio

As already mentioned, the secant stiffness linearization method substitutes to the actual variable structural stiffness a constant value that corresponds to the peak displacement. Displacements close to the peak value are usually attained very few times during seismic response. Therefore this linearization technique underestimates the structural stiffness, and, by a similar argument, overestimates the damping ratio. Lashkari (1992) has carried out an extensive investigation on BI structures comparing the peak displacements obtained by using both nonlinear time history analysis and the secant stiffness method. Specifically, the mean values of the peak displacements obtained by nonlinear time history analysis under different ground motion records scaled to a given peak ground acceleration were compared to the displacements calculated trough secant stiffness linearization. The spectrum used in the latter method was determined by averaging the spectra for the ground motion records. The result of the linearization procedure was found to overestimate the mean displacement value calculated by the time history analyses by 10% to 20%. This result indicates a reasonable accuracy (on the conservative side) of the simplified procedure.

3.3 Equivalent Stiffness Linearization

Kennedy (1989) has proposed a different equivalent linearization procedure to predict the inelastic response of Single Degree Of Freedom (SDOF) structures. The procedure is

K_1 and K_s are, respectively, the elastic and the secant stiffness, and C_f is an empirical coefficient. Kennedy recommends to keep A not greater than 0.85. Since no further suggestions was given about this coefficient, in this thesis, when applying this method, the value 0.85 has been used for A in eq. (3.3) whenever eq. (3.4) gave a greater value.

The equivalent damping ratio given by Kennedy is

$$\beta_{eq} = \frac{K_s}{K_{eq}}\left[\beta_v + C_n\left(1 - \sqrt{\frac{K_s}{K_1}}\right)\right] \tag{3.6}$$

where β_v is the viscous damping ratio and C_n is an empirical coefficient.

The frequency shift coefficient C_f and the hysteretic damping coefficient C_n depend on the duration of the strong portion of the ground motion, as follows:

Strong duration time	Effective number of strong nonlinear cycles	C_f	C_n
< 1.0 sec	1	1.	0.30
1.0 - 7.0 sec.	2	1.	0.15
9.0-11.0 sec	3	2.	0.11
> 15.0 sec	4	2.	0.11

Figure 3.4.a and 3.4b show how the equivalent stiffness and the equivalent damping ratio (β_v=0) depend on the ductility ratio, according to Kennedy (1989). The values of the other parameters are as specified earlier. For comparison, the secant stiffness and the corresponding effective damping ratio are plotted as dashed lines.

Figure 3.4 shows that, for a given ductility ratio greater than one, the secant stiffness is less than the Kennedy's equivalent one, but that, less obviously, the effective damping ratio of the secant rule is much larger than the equivalent one. The same figure shows also the influence on the equivalent values of stiffness and damping ratio of bounding the parameter A. This condition affects the smoothness of the plot in the case of a high number of strong nonlinear cycles. Furthermore, it seems rather unusual to consider the equivalent damping ratio as a decreasing function of the number of strong nonlinear cycles that

3.4 Alternative Methods Based on the Equivalent Stiffness

The results of an extensive numerical investigation dealing with the nonlinear response of SDOF systems characterized by several different hysteretic behaviors carried out by Iwan and Gates (1979) have shown that the response of nonlinear systems in terms of displacements can be predicted by the elastic response of equivalent linear systems. Iwan has also observed a weak dependency of the linearized system properties on the shape of the hysteretic loops of the nonlinear systems. Based upon this observation, Iwan (1980) has derived the equivalent stiffness and damping ratio of the linear system that produces the best fits of the maximum displacements calculated by nonlinear time history analysis of several combinations of systems and ground motions records. This relationships, valid for K_1/K_2 =20, are:

$$\sqrt{\frac{K}{K_{eq}}} = 1 + 0.121\,(\mu - 1)^{0.939} \tag{3.7}$$

$$\beta_{eq} = \beta_v + 0.0587\,(\mu - 1)^{0.371} \tag{3.8}$$

Hwang et al. (1992) have proposed a different expression for the equivalent stiffness, by fitting the maximum displacements of (Iwan, 1980) with an exponential function. Their analysis leads to the following formula:

$$\sqrt{\frac{K}{K_{eq}}} = 1 + \ln\left[1 + 0.13\,(\mu - 1)^{1.137}\right] \tag{3.9}$$

The equivalent damping ratio is calculated by solving eq. (3.8) for (μ-1) and substituting it in eq. (3.7). Figures 3.7a and 3.7b show the equivalent stiffness and damping ratios according to Iwan (1980) and Hwang et al. (1992) (solid lines). For comparison, the secant stiffness and the correspondent effective damping ratio are plotted as dashed lines, and the equivalent stiffness and damping ratio according to Kennedy are shown as dashed-dotted lines. In all cases the ratio K_1/K_2 is equal to 20, and other parameters are as specified earlier.

the stiffness as a function of the shear strain. They have also derived an equivalent linear viscous model for this kind of isolators, providing an analytical expression for equivalent stiffness and damping ratio. Specifically, for a given maximum displacement, the stiffness of the equivalent linear model is set equal to 1.19 times the corresponding value of the exponential fitting function. The numerical analyses presented by these authors closely match the experimental results.

3.5 Modal Analysis of Linearized Base Isolated Structures

Figure 3.6 shows a schematic lumped mass model often used in the dynamic analysis of base isolated shear-type frames. The structure and the isolation layer are represented by masses connected by elastic members and dashpots.

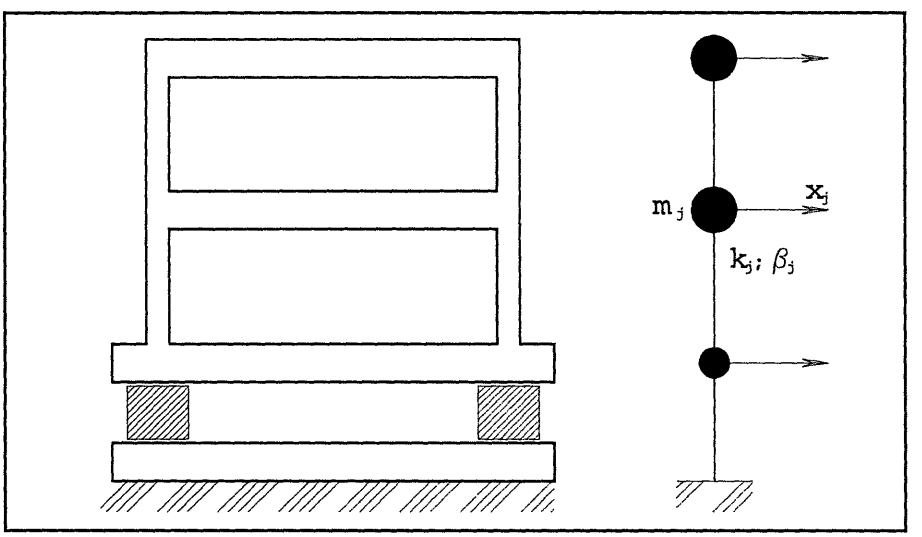

Figure 3.7: Schematic model of B.I. structure

In engineering practice, the viscous damping ratio associated with each structural mode is determined empirically so as to maintain the orthogonality of the modes. Therefore, once a damping ratio is assigned to a given mode (usually the first one), the others are calculated by assuming linear dependence of the damping matrix on the mass and stiffness matrices. The empirically assigned damping ratio, and thus the others, accounts for a combination of viscous and hysteretic damping expected to develop in the structure under

$$\beta_{ieq} = \frac{1}{4\pi} \frac{\sum_{j=1}^{n} \left[\beta_j \frac{\omega_i}{\omega_j} + D_j \right] k_j \Delta_{ij}^2}{\sum_{j=1}^{n} k_j \Delta_{ij}^2} \tag{3.11}$$

in which

- β_j viscous damping ratio of the j-th member at the frequency ω_j;
- ω_j reference frequency
- ω_i frequency of the i-th mode;
- D_j hysteretic damping ratio (loss factor) of the j-th member;
- k_j stiffness of the j-th member;
- Δ_{ij} strain in the j-th member corresponding to the i-th mode.

For the case of only hysteretic damping, equation (3.7) was first proposed by Biggs (1969). Equation (3.7) gives each modal equivalent damping ratio as a weighted average of the energy dissipated by the structural modes, utilizing the corresponding strain energies as weights of the sum.

3) the structural response has been determined by modal superposition using an iterative procedure and one of the linearization rules described in chapter 3; specifically, after calculating the response, the resulting equivalent stiffness and damping ratio of each structural member have been compared to those used in the analysis, iterating the procedure until convergence;

4) the calculations have been repeated by scaling the peak ground acceleration up to achieve a maximum ductility ratio ranging from 0 to 10 in the structure above the isolator layer.

4.2 Ground Motions and Response Spectra

Four different response spectra have been used in the analysis. Three of them have been calculated from actual earthquake records, whereas the fourth is the U. S. Atomic Energy Commission Regulatory Guide 1.60 design spectrum. The ground motion records considered are the NS 1940 Imperial Valley (El Centro) and the NS Calitri and NS Auletta records from the 1980 Irpinia, Italy, earthquake. The associated acceleration time histories, shown in figure 4.2, differ in duration and intensity., and the response spectra, plotted in figure 4.3, differ in smoothness and frequency content. In particular, and with reference to the structures analyzed in this thesis and described in section 4.4, notice that, at the lowest level of damping and in the range 0.3 to 1 s, the spectral shapes have a quite different aspect and, more importantly, decay with different rates as T approaches 1 s. At the highest level of damping and in the range 3 to 4.5 s, all the spectra look smooth, but the ratios of the spectral accelerations at the ends of this range are very different.

These response spectra will hereafter be referenced by letter code as indicated in table 4.1.

Code	Response spectrum
a	Auletta 1980
b	Calitri 1980
c	El Centro 1960
d	U.S. A.E.C. Reg Guide 1.60

Table 4.1: Seismic input codes.

4.3 Isolation systems

The isolation layer is assumed to be made up of identical elastomeric laminated high-damping rubber devices, with circular cross sections and bilinear restoring force. The bearings of a given isolation system are assumed to share equally the vertical and horizontal loads. Parameters that need to be specified are:

The diameter D. As representative cases of small-diameter and large-diameter bearings, the values D=0.50 m and D=0.80 m have been considered;

The total rubber thickness h or, equivalently, the secondary shape factor $S_2=D/h$. Secondary shape factors between 3 and 8 are typically used in practice;

The admissible vertical stress σ for the rubber. Higher values of σ lead to smaller bearings and produce higher natural periods of the isolation system; therefore they are attractive for relatively tall buildings. The values considered in the present analysis are 10 and 30 MPa.

The post-yielding shear modulus of the rubber G. Values of about 0.6 MPa have been determined by identification analyses on bearings currently in use (Serino et al. 1992; Serino et al. 1993). However, developments in the technology of rubber production may soon result in smaller values of G (Takayama and Kitamura, 1992). In

case	# of floors	D [m]	h [m]	S_2	σ [MPa]	G [MPa]	α_y	T [sec]	T^* [sec]
1	3	0.5	0.125	4.01	10	0.4	0.10	0.30	2.5
2	3	0.5	0.080	6.27	10	0.4	0.10	0.30	2.0
3	3	0.5	0.156	3.20	10	0.4	0.10	0.30	2.5
4	3	0.5	0.094	5.33	10	0.2	0.04	0.30	2.5
5	3	0.5	0.083	6.01	30	0.4	0.04	0.30	2.5
6	3	0.8	0.125	4.01	10	0.4	0.04	0.50	2.5
7	10	0.8	0.156	5.12	10	0.4	0.06	0.80	2.5
8	10	0.8	0.183	4.36	10	0.4	0.02	1.20	3.5

Table 4.2: Characteristics of the bearings used in numerical analyses

4.4 Structural systems

Four basically different structures have been analyzed. They differ in the number of stories n (3 or 10) and in the natural period T (0.3 or 0.5 sec for n=3 and 0.8 or 1.2 sec for n=10): see Table 4.2. For each bearing design, the floor masses and the interstory stiffness have been varied to match the bearings' properties. Specifically, the total mass M has been determined from

$$M = \frac{\sigma A}{g} \tag{4.4}$$

whereas the mass above the isolator m_0 and the masses m_i of the various stories have been determined as

$$m_0 = \frac{0.5}{n+0.5} M \tag{4.5}$$

and

$$m_i = \frac{1}{n+0.5} M \tag{4.6}$$

The design strength has been calculated so that the structure yields when the shear strain of the rubber reaches γ^*. The base shear (which is also the strength of the first story) is given by

$$V = F_y + K_2(\delta - \delta_y) = \alpha_y g M \left(1 - \frac{K_2}{K_1}\right) + GA\gamma^*, \tag{4.7}$$

plotting the responses of interest against the scaling factor of the normalized response spectra, λ, expressed in g. In all the analyses, λ varies between 0 and the value that produces a maximum ductility ratio in the structure equal to 10.

Figure 4.4 shows the evolution of the first two modal shapes of base-isolated structure 1 under seismic input c. It is interesting that the first modal shape is very close to that corresponding to that of a SDOF system, in which only the isolation layer is deformed. Comparable strains in the structure and in the isolators are predicted by the second mode, as well as by the highest ones. However, due to the different values of the corresponding participation factors, the results of the modal superposition show that the strain is much greater in the isolation layer than in the structure over a broad range of values of λ. This finding is common to all the structures we have analyzed (for which the ratio T^*/T has been kept between 3 and 8).

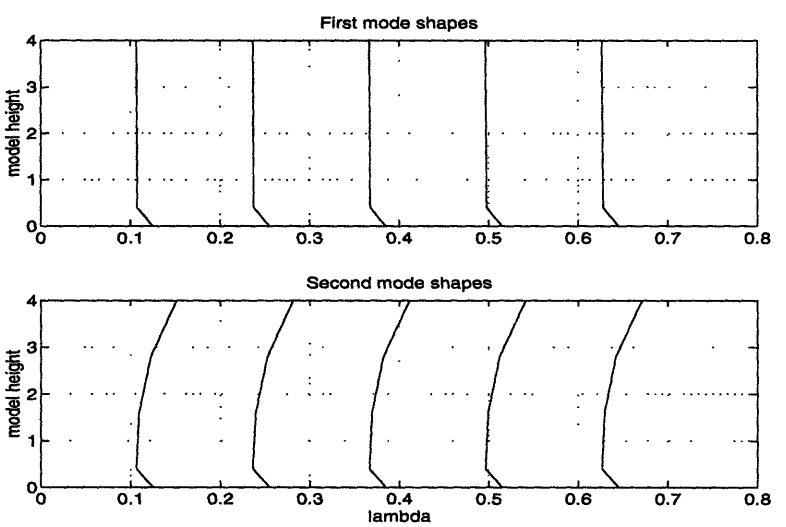

Figure 4.4: Modal shapes, structure 1, seismic input c.

For the same structure and input motion, figures 4.5a and 4.5b show the evolution of the modal periods and the modal participation factors, whereas fig 4.5c and 4.5d show the same parameters calculated for the companion fixed-base structure.

The dashed line in figure 4.5a represents the evolution of T^*, which follows very closely the first period of the BI structure over the whole range of λ. Indeed, the floor dis-

4.6 Numerical Results: Structural Demand

A response parameter of particular interest to us is the "seismic ductility" $R_o(\mu)$, which is defined as the ratio

$$R_o(\mu) = \frac{\lambda(\mu)}{\lambda(\mu_o)} \tag{4.10}$$

where μ is the maximum ductility anywhere in the structure above the isolator layer and $\lambda(\mu)$ is the associated seismic intensity. Therefore R_0 measures the available strength reserve of a structure past the first yielding point. A similar quantity was first introduced by Kennedy (1989) for SDOF systems, and has been later defined for MDOF structures in Bazzurro and Cornell (1992, 1994a, 1994b). Figure 4.6 shows the functions $\mu(\lambda)$ and $R_0(\mu)$ for the 3 story structures with T=0.3 s in the case of response spectrum d. Figure 4.7 shows the same functions for structure 1 and different seismic inputs. Both figures show also results for the companion fixed-base structures. Structures 1 to 5 differ mainly in the design of the isolation system. This is why their respective FB companions structures have similar behavior. Figure 4.6 shows that the ground motion intensity at first yielding is 5 to 10 times higher for the BI structures than for the FB structures. However, the functions $R_0(\mu)$ show a significant reduction in seismic ductility due to base isolation,

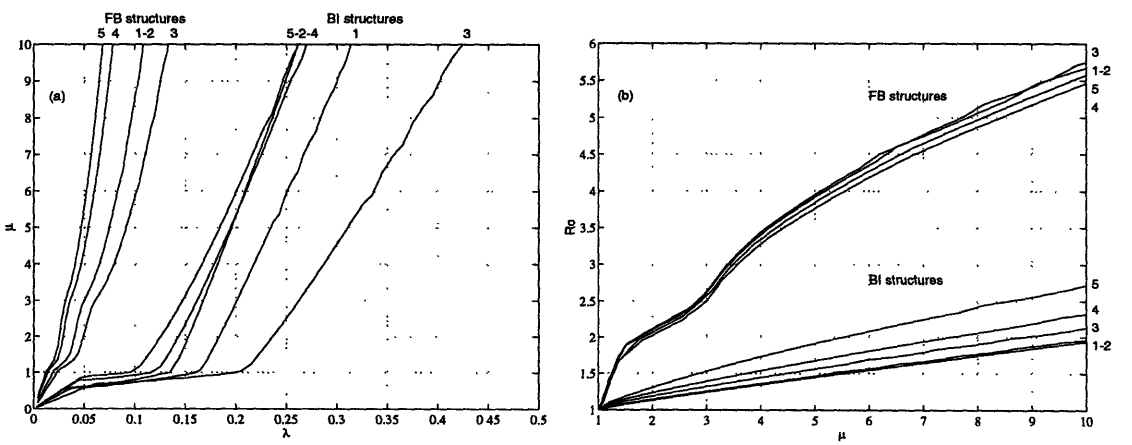

Figure 4.6: Comparison of seismic ductility of FB and BI systems. Structures 1 to 5, seismic input d. (a): $\mu(\lambda)$; (b): $R_0(\mu)$

The peculiar behavior under spectrum a (Auletta) of the BI structure 6 and its FB companion is due to the rapid decay of the spectral acceleration in the period range 2.5-3.0s; analogous but somewhat less pronounced behavior can be seen in figure 4.7 for structure 1.

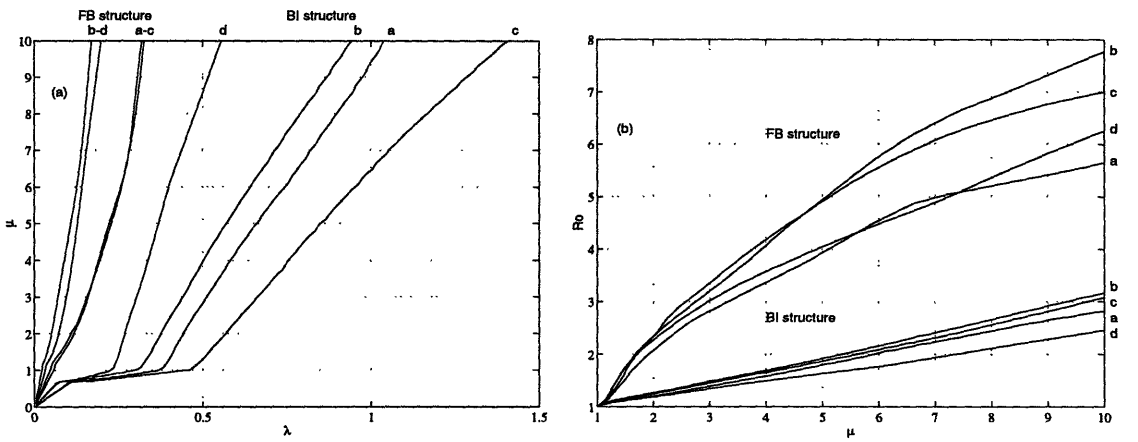

Figure 4.9: Comparison of seismic ductility of FB and BI systems. Structure 7, seismic inputs a to d. (a): $\mu(\lambda)$; (b): $R_0(\mu)$

For FB and BI structures 1, 6, 7 and 8, figure 4.10 shows the development of floor ductilities under seismic input d. Notice that the upper stories of structures 7 and 8 are overdesigned by the method described in section 4.4, whereas the appropiateness of the assumption of equal floor accelerations used to design structures 1 and 6 seems to be verified.

Figure 4.11 shows the functions $\mu(\lambda)$ and $R_0(\mu)$ for modified versions of structure 1, under seismic input d. Specifically, the interstory strength and yielding displacement have been multiplied by a common factor Ψ, while all other parameters have remained unchanged. One can notice that the ductility ratios of the perturbed structures are quite sensitive to T, whereas the seismic ductility is nearly the same.

4.7 Numeric Results: Behavior of the Isolators

Figures 4.6a to 4.9a clearly show the value of λ at which the isolators yield. Figure 4.12 shows the development of shear strain in the isolation layer as a function of the seismic intensity λ for many of the cases analyzed. The curves terminate at the value of λ that corresponds to a maximum ductility ratio in the superstructure equal to 10. In many cases investigated the isolators shear strain after yielding is almost linearly dependent on λ, but this cannot be taken as a general rule, due to the complex and related influence of softening and increased equivalent damping. An accurate definition of the higher period region of the design spectrum becomes therefore a central point in the development of seismic codes for BI structures.

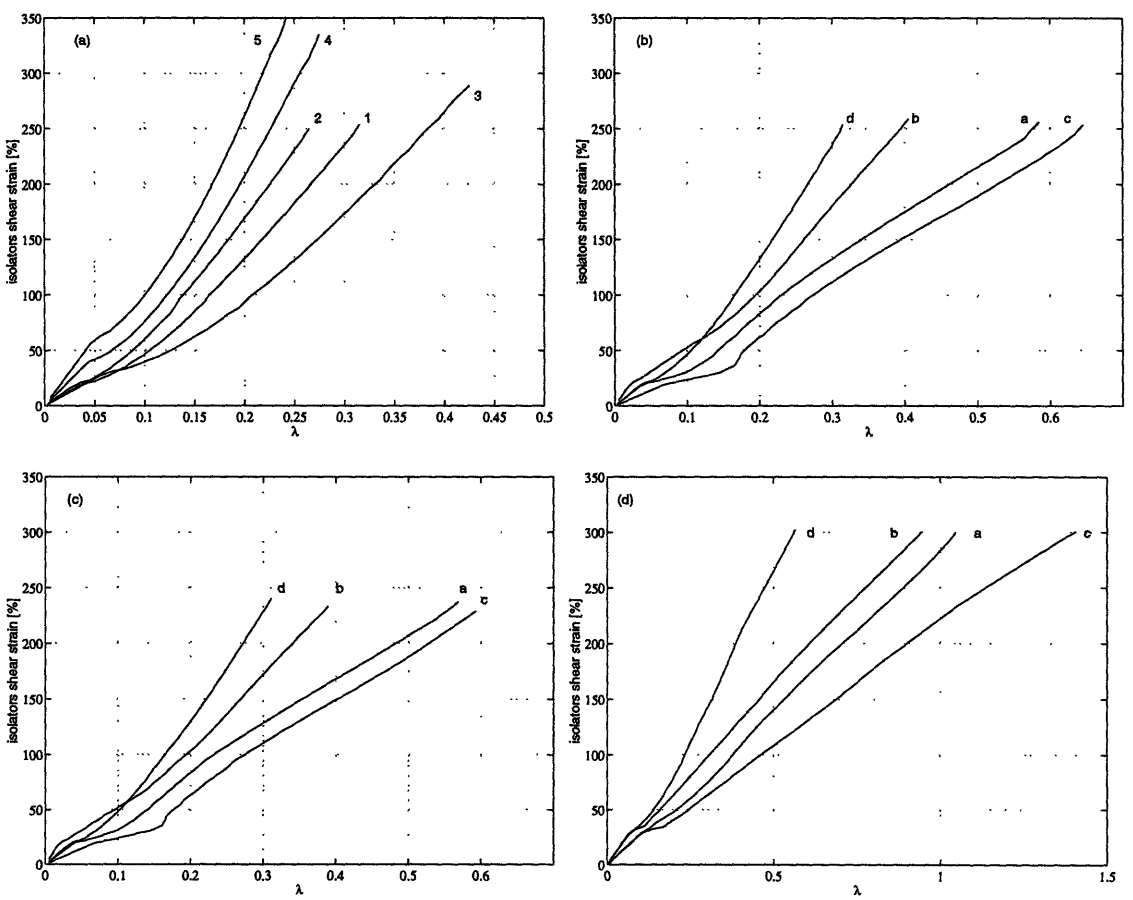

Figure 4.12: Isolators strain vs. λ. (a): structures 1 to 5, seismic input d; (b), (c) and (d): structures 1, 6 and 7, seismic inputs a to d.

Chapter 5

Simplified Approaches to Estimate the Structural Demand and the Seismic Ductility

5.1 A First Simplified Method

For the purpose of safety assessment, it is critical to be able to predict the response of BI structures to ground motions exceeding the design intensity. The choice of the reduction factors, and therefore the design level for BI structures so as to achieve a safety level at least equal to that of FB structures also hinges on this capability. Relative to conventional fixed-base designs, isolated structures can be made to yield at higher ground motion intensity, but once that intensity is exceeded they tend to develop inelastic deformations more rapidly. The lower reduction factor allowed in design codes for BI structures are a consequence of this loss of ductility. This circumstance has been long known (Kaneko et al. 1990; Vestroni et. al. 1991; Lin and Shenton 1992; Calderoni et. al., 1993) and is confirmed by the analyses shown in Chapter 4. In fact, calculation of the functions $\mu(\lambda)$ and $R_o(\mu)$ ordinarily requires detailed nonlinear modelling of the structure/isolation system and tedious computations. The linearization method presented earlier in Chapter 4, which accounts for the contribution of all modes and for the variation of modal periods, damping ratios and shapes as the seismic intensity λ increases, requires a specially written computer code and its practical implementation is restricted to simple MDOF models. This is why we are interested in developing simplified nonlinear analysis procedure

The results presented in figures 4.6 to 4.10 suggest that, in the fairly broad range of combinations of BI structures and seismic inputs considered, the contribution of the higher modes to seismic response is relatively small. Furthermore, once the yielding displacement is exceeded, the slope of $\mu(\lambda)$ is proportional to the value of $\mu(\lambda)$ at first yielding in

Figures 5.2 to 5.5 show the functions $\mu(\lambda)$ and $R_0(\mu)$ obtained with the "accurate" method described in Chapter 4 (solid lines) and using equations (5.1) and (5.2) (dashed lines), for various combinations of structure and seismic input. Notice that, due to the assumptions on the structural properties (simultaneous yielding of all the storeys of the BI structure and constant interstory elastic post-yielding stiffness ratio), the simplified method produces the same functions $R_0(\mu)$ in all cases.

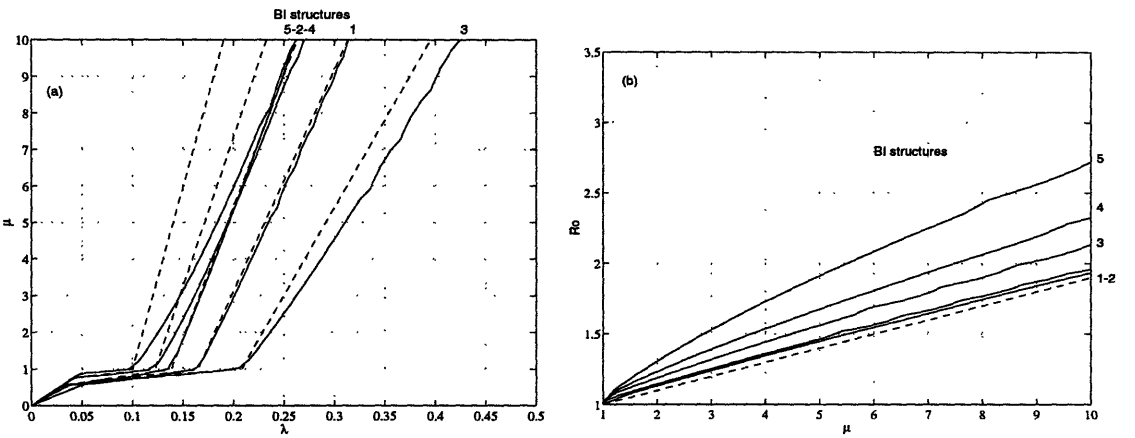

Figure 5.2: Prediction of seismic ductility of BI systems: accurate (solid lines) vs. approximated (dashed lines) methods. Structure 1 to 5, seismic input d. (a): $\mu(\lambda)$; (b): $R_0(\mu)$

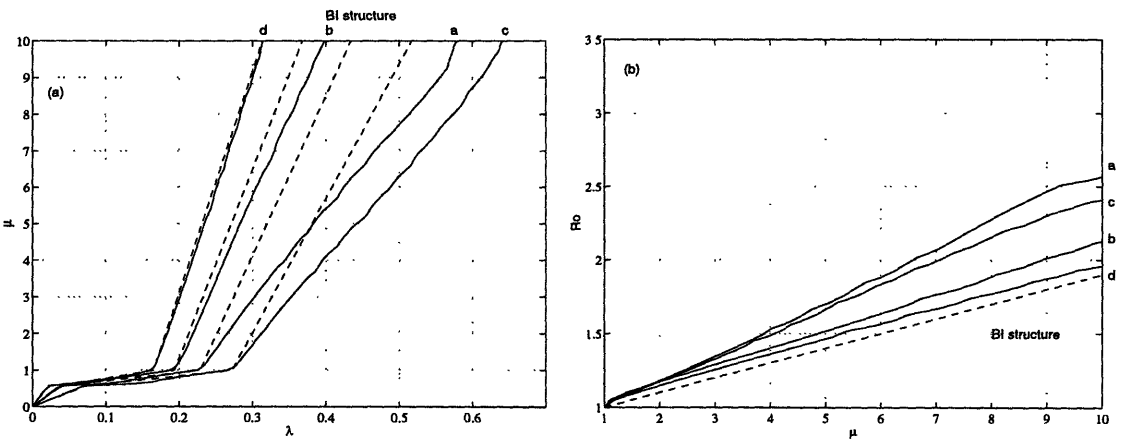

Figure 5.3: Prediction of seismic ductility of BI systems: accurate (solid lines) vs. approximated (dashed lines) methods. Structure 1, seismic inputs a to d. (a): $\mu(\lambda)$; (b): $R_0(\mu)$

For BI structures 1, 6, 7 and 8, figure 5.6 shows the development of floor ductilities, as predicted by the accurate and simplified methods under the Reg. Guide spectrum. The deteriorated performance of the simplified method in the case of structures 8 (and to a lesser extent of structure 7) is due mainly to the decay of the spectral acceleration beyond the design period of the isolator (see table 4.2 and figure 4.3).

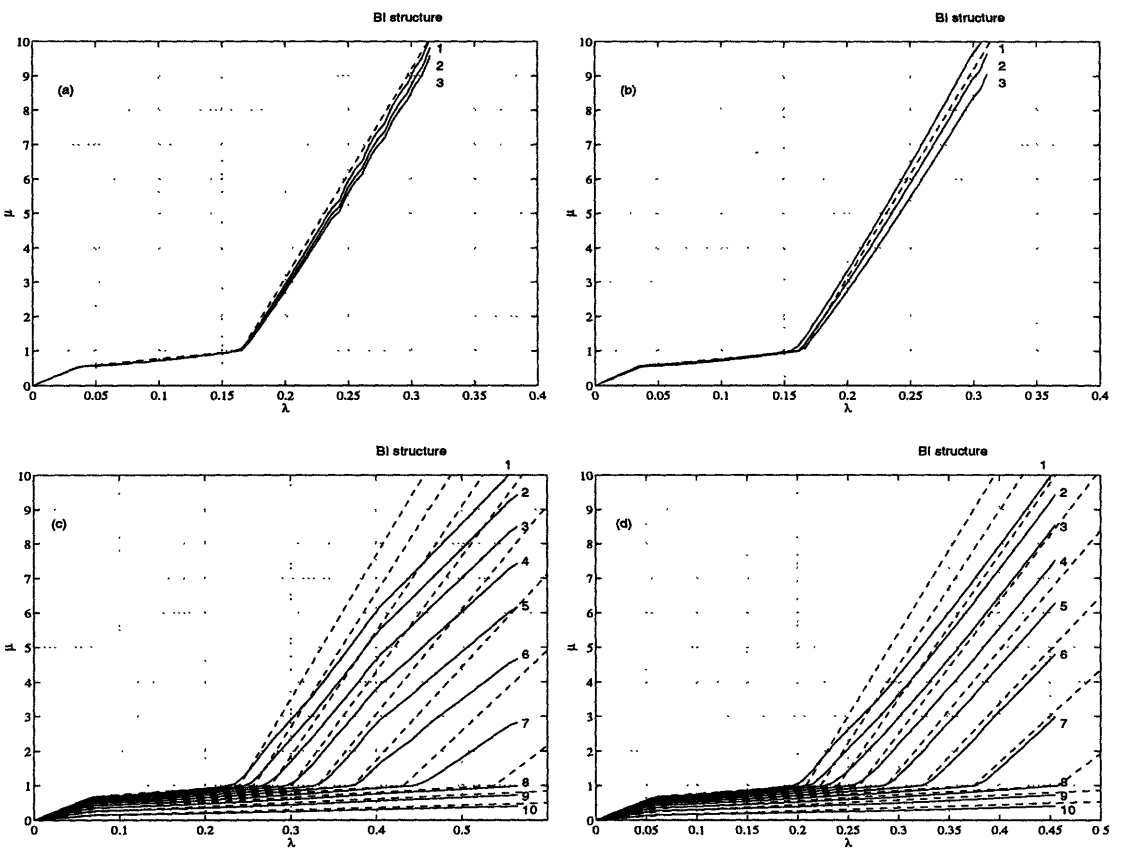

Figure 5.6: Prediction of interstory seismic ductility of BI systems: accurate (solid lines) vs. approximated (dashed lines) methods. Seismic input d. (a): structure 1; (b): structure 6; (c): structure 7; (d) structure 8. The labels refer to the interstory number.

5.2 An Improved Simplified Method

The simplified method works better for stiff superstructures with "well designed" isolation systems, but is less satisfactory for flexible structures and for stiff structures when the isolators undergo large deformations for high value of μ. While several factors may contrib-

In figure 5.7a, the function $\mu(\lambda)$ changes slope at λ=0.4 as a consequence of the change in slope of the response spectrum (from constant velocity to constant displacement). The change occurs at T=4 s, which corresponds to λ about 0.4 (see figure 5.7c).

In both cases considered in figure 5.7, as μ varies from 1 to 10, the first structural period varies between about 3.3 and 4.3 s. Over this range of periods and at high damping ratios the two spectra show a quite different decrease (about 25% for the Reg. Guide spectrum and about 50% for the El Centro spectrum). Equations (5.1) and (5.2) do not account for the variation in spectral acceleration beyond μ=1 and therefore they can be accurate only when this variation is negligible: this is why the approximated method works better with seismic input d.

The approximate method in equations (5.1) and (5.2) can be improved by accounting for the post-yielding change in period T and damping ratio β, while still retaining only the first mode. Accordingly, the functions $\lambda(\mu)$ and $R_0(\mu)$ are given by

$$\lambda(\mu) = \frac{F_{eq}(\mu)}{mS_a(T(\mu), \beta(\mu))} \tag{5.3}$$

$$R_o(\mu) = \frac{F_{eq}(\mu)}{F_{eq}(\mu_o)} \frac{S_a(T^*, \beta^*)}{S_a(T(\mu), \beta(\mu))} \tag{5.4}$$

in which $T(\mu)$ and $\beta(\mu)$ are the (equivalent) fundamental period and damping when the interstory under consideration develops a ductility ratio μ. Figures 5.8 to 5.11 show the functions $\mu(\lambda)$ and $R_0(\mu)$ obtained with the accurate method described in Chapter 4 (solid lines) and using equations (5.3) and (5.4) (dashed lines), for various combinations of structure and seismic input. The accuracy of this improved simplified method is satisfactorily in all the cases analyzed. The function $R_0(\mu)$ expressed by eq. (5.4) provides a simple design tool to assess the structural safety under the maximum credible earthquake.

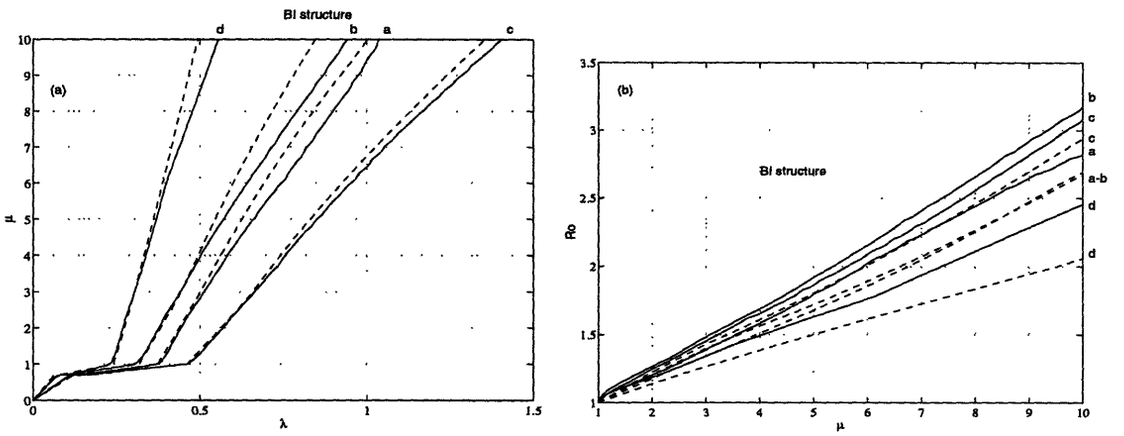

Figure 5.11: Prediction of seismic ductility of BI systems: accurate (solid lines) vs. improved approximated (dashed lines) methods. Structure 7, seismic inputs a to d. (a): $\mu(\lambda)$; (b): $R_0(\mu)$

The estimates provided by equation (5.3) for the function $\mu(\lambda)$ are more accurate than those provided by equation (5.4) for the function $R_0(\mu)$. Equation (5.3) does not account for the dynamic contribution of the superstructure, and therefore, in some case, the value of λ corresponding to first yielding of the superstructure is less accurate, and so is the denominator of equation (5.4).

the interstory, which is then corrected according to an equivalent linearization scheme (see figure 5.1). For the first simplified method, when earthquake intensity is normalized with respect to the value at first yielding, the relationship between inelastic deformation and earthquake intensity becomes independent of the ground motion. Many numerical analyses have shown that this simplified method produces accurate enough and conservative results, especially for stiff structures. For flexible structures the degree of conservatism increases.

4. As a consequence of the same observation, BI structures with sufficiently high ratio T/T^* are insensitive to irregularities in the vertical distribution of stiffness, mass and strength. This lack of sensitivity is reflected in the form of the functions $\lambda(\mu)$ and $R_0(\mu)$ according to the simplified method (masses enter equations (5.1) and (5.2) simply through the m term, strengths are included in the F_{eq} term, and stiffnesses do not appear at all).
5. For BI structures having low to medium ratios T/T^*, we have developed a slightly modified version of the simplified method that accounts for the period shift due to the inelastic deformations of the superstructure and for the corresponding variations of the spectral acceleration. This improved method still produces conservative results but features a much greater accuracy without introducing heavy calculations. The results produced by this improved method, are very accurate in estimating the function $\mu(\lambda)$, and are fairly satisfactorily for the prediction of the function $R_0(\mu)$. Equations (5.3) and (5.4) should be used in the context of preliminary design to assess the safety of BI structures at the MCE level.
6. For shear buildings with bilinear hysteretic interstory behavior, with stiffness ratio K_1/K_2=0.1 and ultimate ductility in the range 3-10, base isolation increases the seis-

References

AASHTO (1992), American Association of State Highway Transportation Officials, *Design Procedure for Seismically Isolated Bridges*, Dynamic Isolation Systems, Inc., Berkeley, California.

Bazzurro P. and Cornell C. A. (1992), *Seismic Risk: Non-linear MDOF Structures*, Proceedings of the 10th World Conference on Earthquake Engineering, Balkema, Rotterdam, The Netherlands.

Bazzurro P. and Cornell C. A. (1994 a), *Seismic Hazard Analysis of Nonlinear Structures. I: Methodology*, to appear in ASCE, Journal of Structural Engineering.

Bazzurro P. and Cornell C. A. (1994 b), *Seismic Hazard Analysis of Nonlinear Structures. II: Applications*, to appear in ASCE, Journal of Structural Engineering.

Bertero V. V. (1986), *Evaluation of Response Reduction Factors Recommended by ATC and SEAOC*, Proceedings of the Third U.S. National Conference on Earthquake Engineering, Charleston, South Carolina.

Bertero V. V. (1988), *Ductility Based Structural Design*, Proceedings of the Ninth World Conference on Earthquake Engineering, Tokyo-Kyoto, Japan.

Biggs (1970), *Structural Response to Seismic Inputs*, in Hansen R. J., editor, Seismic Design for Nuclear Power Plants, The MIT Press, Cambridge, Massachusetts.

Calderoni B., De Crescenzo A., Ghersi A. and Serino G. (1993), *The Design Level for Base Isolated Structures*, Proceedings of the VI National Conference on Seismic Engineering in Italy, Perugia, Italy. (in Italian)

De Luca A., Faella G. and Mele E. (1994), *Effects of Design Level on Dynamic Behavior of Multistory Base Isolated Structures*, Proceedings of II International Conference on Earthquake Resistant Construction and Design, Berlin, Germany.

Hwang J. S., Sheng L. H. and Gates J. H. (1992), *Equivalent Elastic Analysis of Base-Isolated Bridges with Lead-Rubber Bearings*, Proceedings of the ATC-17-1 Seminar on Seismic Isolation, Passive Energy Dissipation and Active Control, San Francisco, California.

Iwan W. D. and Gates N. C. (1979), *The Effective Period and Damping of a Class of Hysteretic Structures*, Earthquake Engineering and Structural Dynamics, vol. 7, 199-211.

Iwan W. D. (1980), *Estimating Inelastic Response Spectra from Elastic Spectra*, Earthquake Engineering and Structural Dynamics, vol. 8, 375-388.

Kaneko M., Tamura K., Maebayashi K. and Saruta M. (1990), *Earthquake Response Characteristics of Base-Isolated Buildings*, Proceedings of the Fourth U.S. National Conference on Earthquake Engineering, Palm Springs, California.

Kelly J. M. (1990), *Base Isolation: Linear Theory and Design*, Earthquake Spectra, vol. 6, n. 2.

Kelly J. M. (1993), *Recent Developments on the Isolation of Civil Buildings in the United States*, Proceedings of the International post-SMiRT Conference Seminar on Isolation, Energy Dissipation and Control of Vibration of Structures, Capri, Italy.